

---

## Nanoencapsulation of Withaferin-A for the Treatment of Neurological Disorder

**Sonu Sharma<sup>1</sup>, Dr. Viney Lather<sup>1\*</sup>, Dr. Vikram Sharma<sup>2</sup>**

<sup>1</sup>Amity Institute of Pharmacy, Amity University, Noida, U.P.,  
sonu.sharma3@student.amity.edu

<sup>1\*</sup>Amity Institute of Pharmacy, Amity University, Noida, U.P.

<sup>2</sup>Galgotia College of Pharmacy, Greater Noida, U.P.

Correspondence Author\*

Dr. Viney lather, Associate professor, vlather@amity.edu, Institute of Pharmacy, Amity University, Noida

Received: 22-March-2022

Revised: 12-May-2022

Accepted: 25-May-2022

### Abstract

A better delivery mechanism is ensured by a superior formulation. This study is since people believe in natural products more than chemical products. Stress is a bad idea that has a detrimental impact on one's mental and physical health. In today's sedentary society, stress is very common. Drugs on the market are chemically produced and can have negative side effects. As a result, numerous studies have been conducted in order to uncover natural materials having anxiolytic characteristics, one of which is phytochemicals. Nanoparticles were used to try to encapsulate the phytochemical Withaferin-A. This phytochemical's bioavailability and water solubility are expected to improve when it is Nano encapsulated. The polymer Poly-(Lactic Acid) was used to Nano encapsulate Withaferin-A, and the creation of nanoparticles was discovered using the solvent displacement method. The concentration of loaded particles was determined using the diphenyl picrylhydrazyl assay.

**Keywords:** Withania Somnifera, Bioavailability, solvent displacement method, Diphenyl picrylhydrazyl Assay, Neurological disorder

### 1. Introduction

Withania somnifera (Indian ginseng) produces a class of naturally occurring steroids known as withanolides, of which withaferin A (WA) is a member. Withaferin-A (WA) is related to withanolides that are a byproduct of Withania somnifera [1].

Numerous pharmacological actions have been thoroughly studied and published, including those that are anti-inflammatory, immunosuppressive, anti-cancer, antioxidant, and anti-epileptic [2]. Furthermore, WA is the first chemical in this cluster to have outstanding potential for regulating neurosis. The neurotic cells are fully destroyed when provided in isolated form or as a basic extract, displaying its neuro-protective function. WA may be a useful neuroprotective treatment for a variety of different neurological conditions, including Parkinson's disease, cerebral infarctions (CI), amyotrophic lateral sclerosis (ALS), reactive gliosis, and neurological conditions linked to HIV [3]. The sole and most significant issue with the newly identified medicines for illnesses of the brain is that they cannot penetrate the blood-brain barrier (BBB). Interesting investigations on WA have demonstrated that WA can cross the BBB. In pre-clinical trials on animal models, the effectiveness of WA has been equivalent whether taken orally or intraperitoneally. In clinical research Phase I including individuals with osteogenic sarcoma, it was discovered that WA is well tolerated by oral administration. Based on newly discovered information about WA, this molecule can be seen as a possible treatment for neurological illnesses and must be further researched. In this section, we discuss briefly the effects of WA as a neuroprotectant in different neurological disorders [4,5].

Natural substances are currently ingested in their entirety, in part, or as a crude extract. This has the drawback of not being uniformly available in the body or released at the allotted time. This lowers the potential profit margin for natural products [6,7]. In terms of bioengineering, research on Drug Delivery systems (DDS) has advanced

extraordinarily, yet there is a necessity for controlled release systems in DDS for natural substances [8]. When in touch for an extended period, polymeric nanoparticles pose problems with in vivo protein interaction, biocompatibility, and immunological reactivity. In comparable, nano formulation's bilayer design of lipid offers degradability, compatibility with immunological, and associated with selective plasma proteome [9,10].

The standard substance WA will be included in a variety of nanovesicle designs, including those made of Eudragit, Tween 80, and PVA in the current study. Drug encapsulation, shape, size, and potential for drug release in vitro and in vivo were all assessed for prepared nano-formulations. The formulation's potential for apoptotic cell death, genotoxicity, anticancer activity, as well as in vivo anticancer investigations, was assessed in terms of cellular interactions. The potential interactions between the polymeric surfactant and the WA that delay WA release in produced Nano formulations were also assessed using molecular modeling [11-12].

## 2. Materials and Methods

### 2.1 Materials

The source of the withaferin A was obtained from Sigma Aldrich in China. Other additional reagents, solvents and chemicals were of analytical quality and came from DIPSAR, New Delhi.

### 2.2 In silico studies

To increase the stability and effectiveness of the created formulation and improve medication's drug release by in-vitro.

#### a. Quantitative estimation of drug-likeness (QED).

Lipinski's rule of five (RO5), the greatest fundamental theory based on the physical and chemical characteristics of the developments, was used to derive the drug-likeness value, which served as the foundation for the QED. The rule of 3, the Gleeson, Hughes, Ghose, and Veber rules of drug-likeness were only a few of the different perceptions of drug-likeness that were pushed by the RO5, but none of them were adequate to give complete drug similarity. The acceptability-based QED approach is a relatively recent technique. The molecular descriptors lipophilicity (ALOGP), numeral of H-bond acceptors (HBAs), numeral of rotatable bonds, numeral of H-bond donors (HBDs), polar surface area (PSA), and molecular weight (M), were all intended using the Dragon program (ROTBs).

The Open Babel software's SMARTS design was used to count the structural ALERTS in each molecule, and the python computer script was then applied to measure the quantum efficiency of the compounds listed by Bickerton et al. [13].

**Table 1 - Comparison of the examined compounds using Lipinski's rule of five**

Properties	Lipinski's criteria	Withaferin A
Molecular weight.	$\leq 500$ D	470.6
CLog P	$\leq 5$	5.23
Hydrogen bond donor	$\leq 5$	2
Hydrogen bond acceptor	$< 10$	3
Polar surface area	$< 140$ A <sup>2</sup>	39.133
Drug likeness		Passed

#### b. Using the Extended Lipinski's Rule of Five, evaluate the similarity of a drug:

In order to attain the estimates of drug-similarity, the recommendations have devised a number of allowances, including partition coefficient that is log P in the variety of 0.4 to +5.6; molecular weight varies from 180 to 500, and molar refractivity varies from 40 to 130. 20 to 70 atoms (containing H-bond acceptors (e.g., Ns and Os) and donors (e.g., OHs and NHs), with a maximum polar surface area of 140 A<sup>2</sup> [14-15].

However, it's important to highlight the rules' restrictions: Only composites administered orally are subject to the "Rule of Five." Another common strategy for identifying "drug-like" elements is to "acquire from history,"

which requires looking through databases of known mixtures with living processes and making inferences from them.

**Table 2: Comparison of the examined compounds using the expanded Lipinski rule of five**

Properties	Lipinski's criteria	Withaferin A
Number of atom	20-70	37
Molar Refractivity	40-130	111
Total polar surface area	< 140	39.133
Drug likeness		Passed

### c. Absorption, distribution, metabolism, and toxicity features in silico prediction

#### Chemical properties

The compounds in the data are fewer than 500 g/mol in molecular weight, and the majority of these contain a larger numeral of RBN—amid 4 and 7—which indicates rotational flexibility. The significant chemical property of hydrogen bonding is used to characterize the permeability of medicines.

The bulk of the derivates had between 3 and 7 acceptors and fewer donors, as shown in Table 3, in terms of hydrogen bonding. A ligand's lipophilicity can be measured using Log K or Log P. The findings showed that the compounds had low Log p values, indicating high bioavailability. The compounds also had a substantial QED value [16-17].

**Table 3. Molecular parameters**

Compound	MW	ALOGP	nHAcc	nHDon	TPSA(NO)	RBN	nCIC	QED
Withaferin A	470.6	5.23	3	2	39.13	4	4	0.524

nCIC stands for several cyclic rings, nHAcc for the count of H-bond acceptors, NHDOn for the numerals of H-bond donors, and RBN for the count of rotatable bonds. ALogP stands for the logarithm of the drug partition coefficient of water and n-octanol. TPSA stands for topological polar surface area.

#### Comparing a medicine's resemblance to a reference drug quantitatively

Table 4 demonstrates that the test compound's QED values were 0.524 against 0.314 for the standard medication (aspirin).

**Table 4: Expected QED values for problematic medicines**

Compounds	QED
Withaferin A	0.524
Reference drug	0.314

### 3. Setting Up In-Silico ADME and Toxicity Investigations

The important aspects of every test compound's absorption, distribution, metabolism, elimination, and toxicity (ADMET) were analyzed using ADMET SAR software, which has over 210000 ADMET data points.

A database of about 96 000 different compounds and 45 different categories of ADMET-joined features may be found in the open-source ADMET SAR program. The database's excellent predictive performance, needed to estimate ADMET properties, is related to 5 quantitative regression analyses and 22 qualitative categories. [19]

The findings of the ADMET SAR program, which was used to forecast the test compound's absorption, metabolism, and toxicity, are displayed in Table 5. Both the test substance's toxicity and carcinogenicity were determined to be zero.

**Table 5 estimation of Withaferin A toxicity, absorption, and metabolism, via In silico**

		Withaferin A
<b>Absorption</b>	BBB	+
	HIA	+
	Caco-2 permeability	+
	P-GPS	NS
	pGPI	NI
<b>Metabolism</b>	CYP450 2C9	NS
	CYP450 2D6	NS
	CYP450 3A4	NS
	CYP450 1A2	NI
	CYP450 2C9	I
	CYP450 2D6	NI
	CYP450 2C19	I
	CYP450 3A4	I
<b>Carcinogenicity &amp; Mutagenicity</b>	AMES Toxicity	NT
	Carcinogen	NC

BBB stands for blood-brain barrier; HIA stands for human intestinal absorption; p-GPI stands for P-glycoprotein inhibitor; p-GPS stands for P-glycoprotein substrate; NT for nontoxic; T stands for toxic; and NC stands for non-carcinogenic.

#### 4. Preformulating Study

##### 4.1 Preliminary Solubility

The 3-most important characteristics for a molecule to succeed are solubility, permeability, and stability. The preliminary in-silico investigations were used to infer the information on solubility and permeability. This background knowledge will help carry out the real applied study. Active oral compounds must have the least permeability and solubility of 0.1 mg per ml and a  $P_{eff} > 2 \times 10^{-4}$  cm per sec. Therefore, Table 6 demonstrates that neither the test drug nor the standard medication will have a permeability or solubility issue that is similar to influencing its oral administered bioavailability [20-21].

**Table 6 shows the estimated permeability and solubility values.**

Compounds	Solubility( $\mu\text{g}/\text{mL}$ ) by (ADMET Predictor)
Withaferin A	29.3
Reference drug	18.9

##### 4.2 Withaferin A $pK_a$ values:

The  $pK_a$  number is the pH at which both the 1ionized and 1ionized11d forms are present in equal proportions. A compound's  $pK_a$  value provides information on how 1ionized it is in the gastrointestinal system (GIT).

Because  $pK_a$  controls solubility, it may be used to forecast where absorption will occur in the GIT. ADMET Predictor and PALLAS were the two programs we used to predict  $pK_a$  in silico. [22-23]

Since these molecules are inherently unstable in water, it may be required to transform them into respective salts in order to increase their stability. This calls for the computation of both compounds'  $pK_a$  values. The  $pK_a$  of the counter ion should be at the tiniest 2 to 3, indicating that a greater  $pK_a$  is preferable for salt synthesis. Depending on the  $pK_a$  values, an acid or a base can be employed to transform the compound into a salt (stable).

**Table 7 - Projected value of pK<sub>a</sub>**

Compounds	Withaferin A
pK <sub>a</sub> (PALLAS)	6.5(acidic), 1.36(basic)
Acidic pK <sub>a</sub> (ADMET Predictor)	9.12
Basic pK <sub>a</sub> (ADMET Predictor)	-.77

#### 4.3 Withaferin A nanoparticle preparation using a factorial design

The most important parameters and their ranges were identified during the initial screening.

300–1200 mg polymer content

20 to 60 kHz is the sonication frequency.

Time for sonication: 15 to 60 minutes

Early experiments were utilized to create a 3-factor, and 3-level with Box-Behnken drawing to examine every independently variable's impact on the dependent variables (entrapment efficiency, practical yield, and particle size) [24].

#### Dependent variables and independent variables for Withaferin A nanoparticle in Box-Behnken design

Factor	Name	Units	Minimum	Maximum
A	Polymer	mg	300	1200
B	Sonication time	min	15	60
C	Sonication frequency	kHz	20	60

Response	Name	Units
R1	Particle size	nm
R2	Entrapment efficiency	%
R3	Practical yield	%

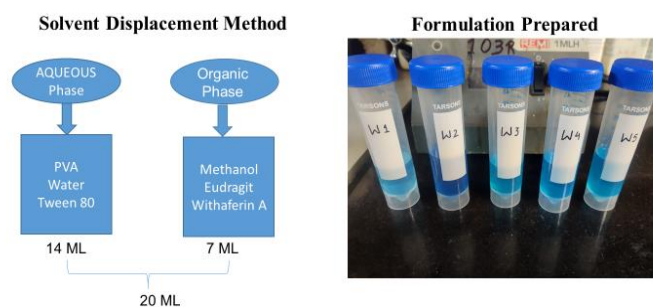
#### 4.4 Formulations Ratio

S.No	Eudragit	PVA	Tween 80	Sriring Speed
1	1.5%-300 mg	0.5%-100mg	2%-600µl	500
2	1%-200 mg	0.5%-100mg	2%-600µl	850
3	1.5%-300 mg	1%-200 mg	2%-600µl	850
4	1.5%-300 mg	1.5%-300mg	2%-600µl	500
5	1%-200 mg	1%-200 mg	2%-600µl	1200
6	1.5%-300 mg	1%-200 mg	2%-600µl	850
7	1%-200 mg	1.5%-300mg	2%-600µl	850
8	2%-400 mg	1%-200 mg	2%-600µl	500
9	1.5%-300 mg	1.5%-300 mg	2%-600µl	1200
10	1.5%-300 mg	1%-200 mg	2%-600µl	850
11	1.5%-300 mg	1%-200 mg	2%-600µl	850
12	1.5%-300 mg	1%-200 mg	2%-600µl	850
13	1%-200 mg	1%-200 mg	2%-600µl	500
14	2%-400 mg	0.5%-100mg	2%-600µl	850
15	2%-400 mg	1%-200 mg	2%-600µl	1200
16	1.5%-300 mg	0.5%-100mg	2%-600µl	1200
17	2%-400 mg	1.5%-300mg	2%-600µl	850

#### 4.5 Drug-loaded nanoparticles formulation development

##### Nanoparticles preparation:

To make the nanoparticles, a revised solvent displacing approach was employed. The setting chosen was 25 °C. The quasi-organic solvent was used to dissolve the bioactive molecules, that is WA. This solution containing the active component was introduced into the aqueous medium using a specific setup while it was being agitated at 500 rpm on a magnetic stirring. At a frequency ranging from 20 to 60 kHz, an ultra-probe sonication was performed for various lengths of time. The measurements were done immediately after the sonication in triplicate. To finish the precipitation process, 200 mL of purified water was mixed and constantly swirled for 12 hrs. on the instrument magnetic stirrer. A Rota-evaporator operating at 40°C was used to vaporize the organic solvent. To make the powder flow unresisted, the resultant nanoparticles were freeze-dried at -20°C for 26 hours [25-26].



##### Prepared Niosome Characterization

#### 4.6 FTIR spectroscopy

FTIR spectrum of our WA pharmaceutical compound, active drug-packed nanosomes, and non-drug packed nano-formulation are obtained using the potassium bromide (KBr) disc technique (lyophilized). To create the pellet for examination, 2% of the material was combined with KBr. To obtain the spectra, a Nicolet 101 Avatar 370 FTIR was employed. The device's speed bandwidth ranges from 4000 to 400 cm<sup>-1</sup> [27].

#### 4.7 Analysis of differential scanning calorimetry (DSC)

To determine the steadiness of the active compound WA in nanoforms, thermal analyses of WA, freeze-dried WA-Nanoforms, and drugs without packed nano-formulation were carried out. To prevent oxidation, a continual flow of N<sub>2</sub>-gas at a speed of 2 ml per min was introduced, and the central heating temperature was set at 10°C/min. DSC 214 Polymer NETZSCH (GmbH Germany) by warming the arrangement to 300°C and applying an unfilled aluminum pan as a standard, the DSC scan was acquired for every sample [28].

### 5. Analysis of SEM

The SEM investigation was performed using the instrument Hitachi S-4700 SEM, which needed to speed up the voltage of 10–20 kV. After processing, the sample was instantly put onto sterile silicon wafers and distributed in ethanol. The samples were gold-sputter-coated for transmission.

#### 5.1 Analysis of Particle size

The vesicle size and distribution were measured using the instrument dynamic light scattering (DLS). For DLS analysis, a 5 mg sample of each lyophilized product was prepared in one milliliter of ultra-pure water or UPW. Zeta potential and hydrodynamic width were assessed using the Malvern Zetasizer Nano as well.

To evaluate the entrapment efficiency (EE) of every formulation, a technique that has been labeled before was modified somewhat. A 100 ml volume of pH 7.4 PBS was used to submerge a dialysis membrane that had been pierced with 2 ml of the Nanoform dispersion. The membrane was then left at room temperature for an hour while being stirred by a magnetic stirrer at 200 rpm. The sample was carefully diluted before the absorbance at 338 nm was evaluated through the instrument UV-Visible spectrophotometer. EE was intended by the given equation [29-30].

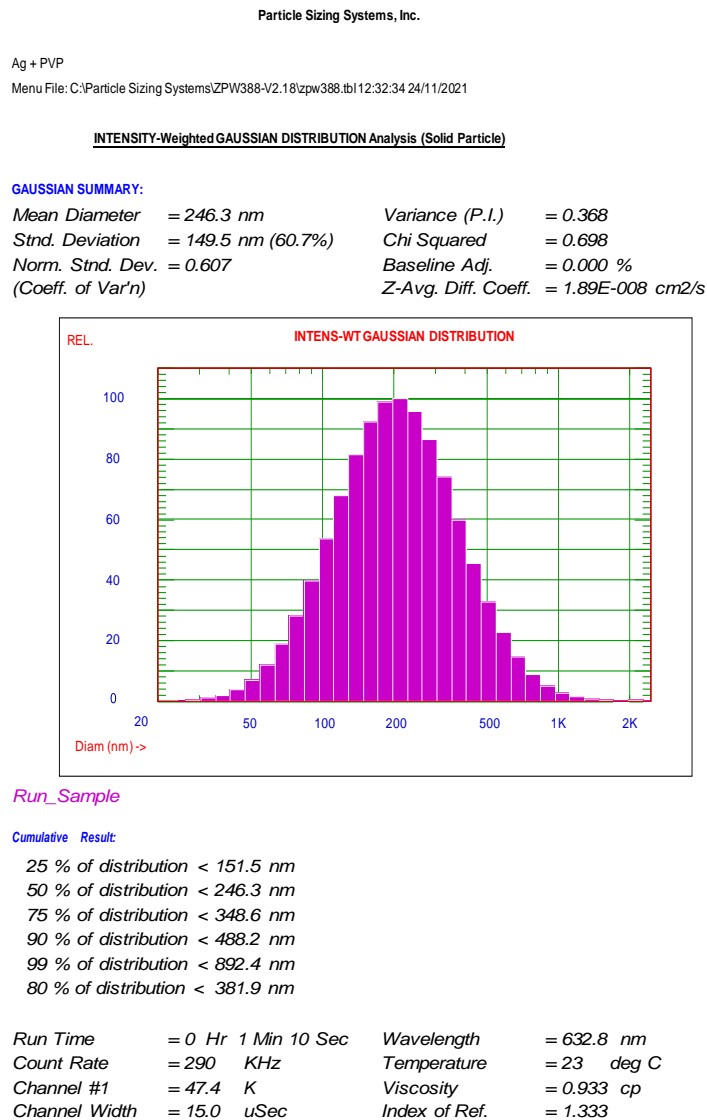
$$EE (\%) = \frac{W2 - W1}{W1} \times 100$$

## 5.2 Dissolution studies in In vitro

Before being placed onto the dialysis membrane, nanoforms (equivalent to 100/21.27 mg per mM of pure medication) were lyophilized and evenly dispersed in 5 ml of pH 7.4 PBS (10K MWCO). To mimic in vivo circumstances, 500 ml of PBS supplemented with lysozyme (1.2 g/ml) were added to the dialysis tube. The experiment was run on a magnetic stirrer at a temperature of 37°C and a speed of 75 revolutions per minute. A UV-Visible instrument was applied to analyze the drug release from the samples after a predetermined amount of time. To ascertain the process of releasing WA, the produced data was examined using 0 order, 1<sup>st</sup> order, Korsmeyer-Peppas, and Higuchi theories with the use of DD solver software [31].

## 5.3 Zeta potential and particle size

A Zeta sizer 300 HS Malvern Instruments from the UK was used to calculate the nanoparticles size. 2 mg of the specimens were dissolved in 2 mL of purified water and nanoparticles size was calculated at 25 °C temp. The diameter of the nanoparticles was measured using the autocorrelation of the brightness of light dispersed by the nanoparticles. These results were assessed three times. The Malvern Analytical Zeta Sizer Nano Particle Detector was used to detect the zeta potential via electrostatic or charge aversion [32-33].



W1 zeta DPSRU

Particle Sizing Systems, Inc.

#1210304, ZRS Freq Mode Don  
 Menu File: C:\Particle Sizing Systems\ZPW388-V2.18\zpw388.tbl 14:18:29 24/11/2021  
 Data Saved: C:\PSS Data 2021\India Demo Z3000\#1210304\ZRS Freq-Don.497



Sample Frequency:	----
Reference Frequency:	----
Cell Current:	0.00 mA
Avg. Phase Shift:	-1.56 rad/Sec.
Avg. Mobility:	0.03 M.U.
Half-Width Mobility Dist:	----
Avg. Zeta Potential:	0.41 mV
Half-Width Zeta Potl Dist:	----
Sample Temperature:	23 C
Liquid Viscosity:	0.890 cPoise
Index of Refraction:	1.333
Dielectric Constant:	78.500
Laser Wavelength:	632.8 nm
Scattering Angle:	-14.1 deg
E-Field Strength:	15.25 V/CM
Channel Width:	20.0 uSec.
Run Time:	00:01:02

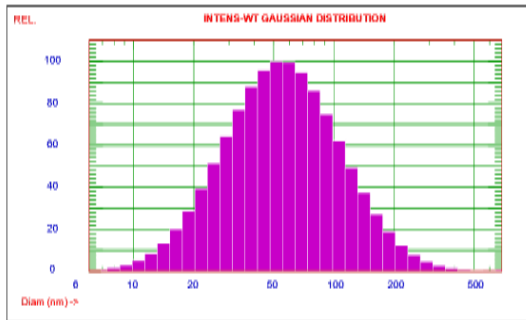
W2 DPSRU

Particle Sizing Systems, Inc.

Ag + PVP  
 Menu File: C:\Particle Sizing Systems\ZPW388-V2.18\zpw388.tbl 12:39:27 24/11/2021

INTENSITY-Weighted GAUSSIAN DISTRIBUTION Analysis (Solid Particle)

<b>GAUSSIAN SUMMARY:</b>			
Mean Diameter	= 68.8 nm	Variance (P.I.)	= 0.456
Std. Deviation	= 46.5 nm (67.5%)	Chi Squared	= 7.653
Norm. Std. Dev.	= 0.675	Baseline Adj.	= 0.018 %
(Coeff. of Var'n)		Z-Avg. Diff. Coeff.	= 6.75E-008 cm <sup>2</sup> /s



Run\_Sample

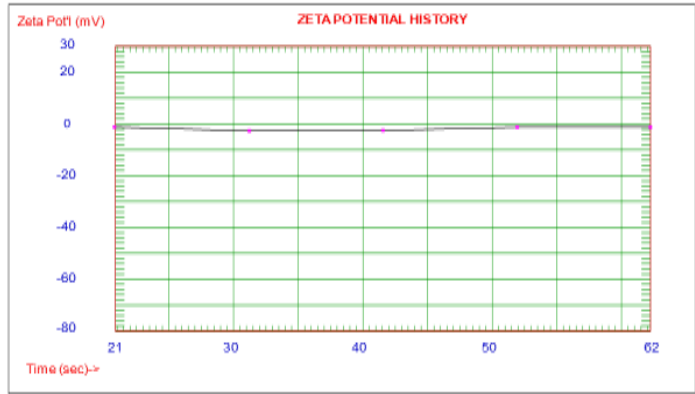
Cumulative Result:  
 25 % of distribution <= 39.7 nm  
 50 % of distribution <= 68.8 nm  
 75 % of distribution <= 100.6 nm  
 90 % of distribution <= 145.7 nm  
 99 % of distribution <= 283.1 nm  
 80 % of distribution <= 111.2 nm

Run Time	= 0 Hr 1 Min 10 Sec	Wavelength	= 632.8 nm
Count Rate	= 311 KHZ	Temperature	= 23 deg C
Channel #1	= 53.5 K	Viscosity	= 0.933 cp
Channel Width	= 15.0 uSec	Index of Ref.	= 1.333

W2 zeta DPSRU

Particle Sizing Systems, Inc.

#1210304, ZRS Freq Mode Don  
 Menu File: C:\Particle Sizing Systems\ZPW388-V2.18\zpw388.tbl 13:46:31 24/11/2021  
 Data Saved: C:\PSS Data 2021\India Demo Z3000#1210304\ZRS Freq-Don.494



Sample Frequency:	----
Reference Frequency:	----
Cell Current:	0.00 mA
Avg. Phase Shift:	4.72 rad/sec.
Avg. Mobility:	-0.10 M.U.
Half-Width Mobility Dist:	----
Avg. Zeta Potential:	-1.23 mV
Half-Width Zeta Potl Dist:	----
Sample Temperature:	23 C
Liquid Viscosity:	0.890 cPoise
Index of Refraction:	1.333
Dielectric Constant:	78.500
Laser Wavelength:	632.8 nm
Scattering Angle:	-14.1 deg.
E-Field Strength:	15.25 V/CM
Channel Width:	20.0 uSec.
Run Time:	00:01:02

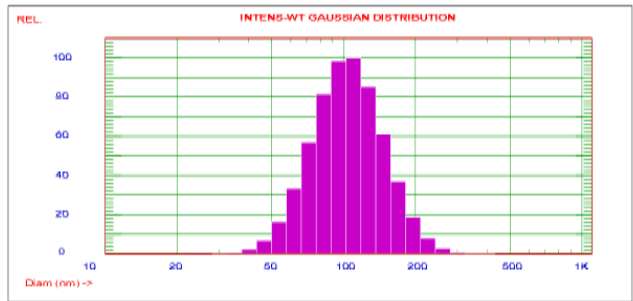
W3 DPSRU

Particle Sizing Systems, Inc.

Ag + PVP  
 Menu File: C:\Particle Sizing Systems\ZPW388-V2.18\zpw388.tbl 12:36:24 24/11/2021

**INTENSITY-Weighted GAUSSIAN DISTRIBUTION Analysis (Solid Particle)**

<b>GAUSSIAN SUMMARY:</b>			
Mean Diameter	= 110.1 nm	Variance (P.I.)	= 0.120
Std. Deviation	= 38.1 nm (34.6%)	Chi Squared	= 0.261
Norm. Std. Dev.	= 0.346	Baseline Adj.	= 0.022 %
(Coeff. of Var'n)		Z-Avg. Diff. Coeff.	= 4.22E-008 cm <sup>2</sup> /s



**Run\_Sample**

**Cumulative Result:**  
 25 % of distribution = 65.1 nm  
 50 % of distribution = 110.1 nm  
 75 % of distribution = 136.2 nm  
 90 % of distribution = 166.2 nm  
 99 % of distribution = 236.4 nm  
 80 % of distribution = 143.8 nm

Run Time	= 0 Hr 0 Min 30 Sec	Wavelength	= 632.8 nm
Count Rate	= 304 KHz	Temperature	= 23 deg C
Channel #1	= 22.3 K	Viscosity	= 0.933 cp
Channel Width	= 15.0 uSec	Index of Ref.	= 1.333

W3 zeta DPSRU

Particle Sizing Systems, Inc.

#1210304, ZRS Freq Mode Don  
 Menu File: C:\Particle Sizing Systems\ZPW388-V2.18\zpw388.tbl 13:58:36 24/11/2021  
 Data Saved: C:\PSS Data 2021\India Demo Z3000#1210304\ZRS Freq-Don.496



Sample Frequency:	----
Reference Frequency:	----
Cell Current:	0.00 mA
Avg. Phase Shift:	-2.06 rad/sec.
Avg. Mobility:	0.06 M.U.
Half-Width Mobility Dist:	----
Avg. Zeta Potential:	0.09 mV
Half-Width Zeta Potl Dist:	----
Sample Temperature:	23 C
Liquid Viscosity:	0.890 cPoise
Index of Refraction:	1.333
Dielectric Constant:	78.500
Laser Wavelength:	632.8 nm
Scattering Angle:	-14.1 deg
E-Field Strength:	15.25 V/CM
Channel Width:	20.0 uSec.
Run Time:	00:01:02

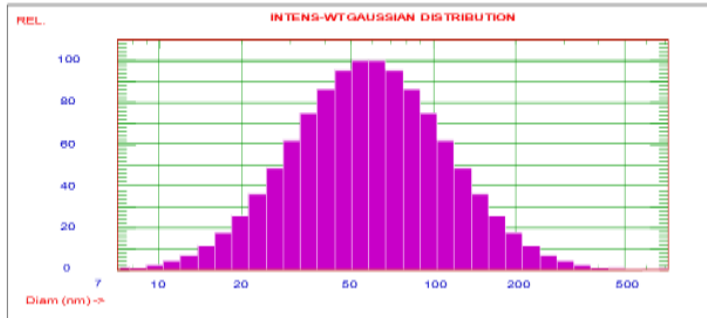
W4 DPSRU

Particle Sizing Systems, Inc.

Ag + PVP  
 Menu File: C:\Particle Sizing Systems\ZPW388-V2.18\zpw388.tbl 12:42:23 24/11/2021

**INTENSITY-Weighted GAUSSIAN DISTRIBUTION Analysis (Solid Particle)**

<b>GAUSSIAN SUMMARY:</b>			
Mean Diameter	= 72.2 nm	Variance (P.I.)	= 0.430
Std. Deviation	= 47.4 nm (65.6%)	Chi Squared	= 5.789
Norm. Std. Dev.	= 0.656	Baseline Adj.	= 0.008 %
(Coeff. of Var'n)		Z-Avg. Diff. Coeff.	= 6.44E-008 cm <sup>2</sup> /s



**Run\_Sample**

**Cumulative Result:**  
 25 % of distribution = 42.4 nm  
 50 % of distribution = 72.2 nm  
 75 % of distribution = 104.6 nm  
 90 % of distribution = 150.1 nm  
 99 % of distribution = 286.8 nm  
 80 % of distribution = 115.3 nm

Run Time	= 0 Hr 1 Min 10 Sec	Wavelength	= 632.8 nm
Count Rate	= 327 KHz	Temperature	= 23 deg C
Channel #1	= 57.5 K	Viscosity	= 0.933 cp
Channel Width	= 13.0 uSec	Index of Ref.	= 1.333

W4 zeta DPSRU

Particle Sizing Systems, Inc.

#1210304, ZRS Freq Mode Don  
 Menu File: C:\Particle Sizing Systems\ZPW388-V2.18\zpw388.tbi 13:40:42 24/11/2021  
 Data Saved: C:\PSS Data 2021\India Demo Z3000#1210304\ZRS Freq-Don.493



Sample Frequency:	----
Reference Frequency:	----
Cell Current:	3.33 mA
Avg. Phase Shift:	-9.81 rad/sec.
Avg. Mobility:	0.20 M.U.
Half-Width Mobility Dist	----
Avg. Zeta Potential:	2.55 mV
Half-Width Zeta Potl Dist.	----
Sample Temperature:	23 C
Liquid Viscosity:	0.890 cPoise
Index of Refraction:	1.333
Dielectric Constant:	78.500
Laser Wavelength:	632.8 nm
Scattering Angle:	-14.1 deg
E-Field Strength:	15.25 V/CM
Channel Width:	20.0 uSec.
Run Time:	00:01:02

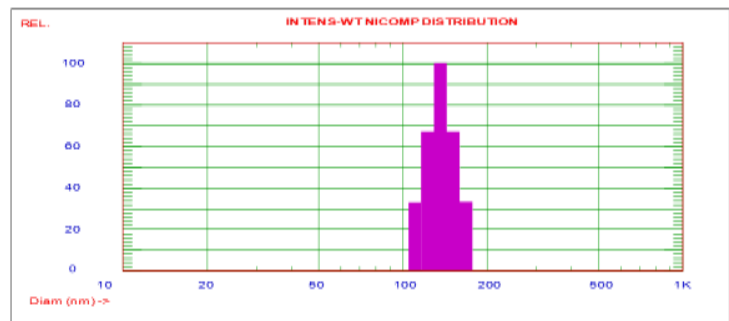
W5 DPSRU

Particle Sizing Systems, Inc.

Ag + PVP  
 Menu File: C:\Particle Sizing Systems\ZPW388-V2.18\zpw388.tbi 12:18:37 24/11/2021  
 Data Saved: C:\PSS Data 2017\Reena\Ag.pvp.38

INTENSITY-WEIGHTED NICOMP DISTRIBUTION Analysis (Solid Particle)

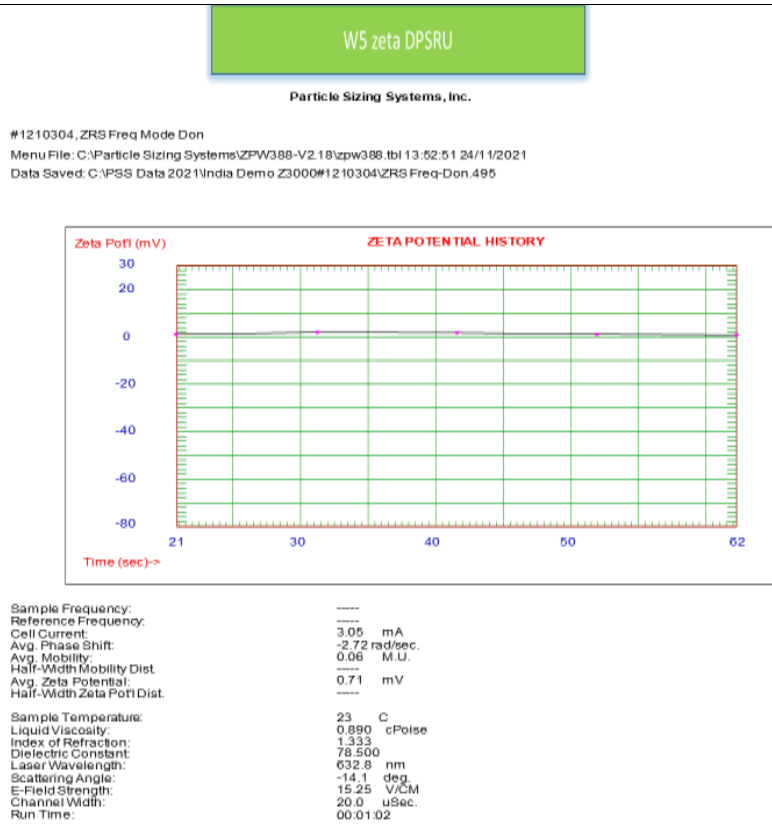
NICOMP SUMMARY:  
 Peak #1: Mean Diam.= 127.9 nm, S.Dev.= 19.7 nm (12.5%) Intens.= 100.0 %



Ag.pvp.38  
 Mean Diameter = 137.9 nm Fit Error = 473.571 Residual = 0.000

NICOMP SCALE PARAMETERS:  
 Min. Diam. = 10 nm Plot Size = 45  
 Smoothing = 3 Plot Range = 100

GAUSSIAN SUMMARY:			
Mean Diameter	= 187.4 nm	Variance (P.I.)	= 1.036
Std. Deviation	= 190.8 nm (101.8%)	Chi Squared	= 10.882
Norm. Std. Dev.	= 1.018	Baseline Adj.	= 0.000 %
(Coeff. of Var'n)		Z-Avg. Diff. Coeff.	= 2.48E-008 cm2/s
Run Time	= 0 Hr 3 Min 38 Sec	Wavelength	= 632.8 nm
Count Rate	= 9 KHz	Temperature	= 23 deg C
Channel #1	= 0.1 K	Viscosity	= 0.933 cp
Channel Width	= 15.0 uSec	Index of Ref.	= 1.333



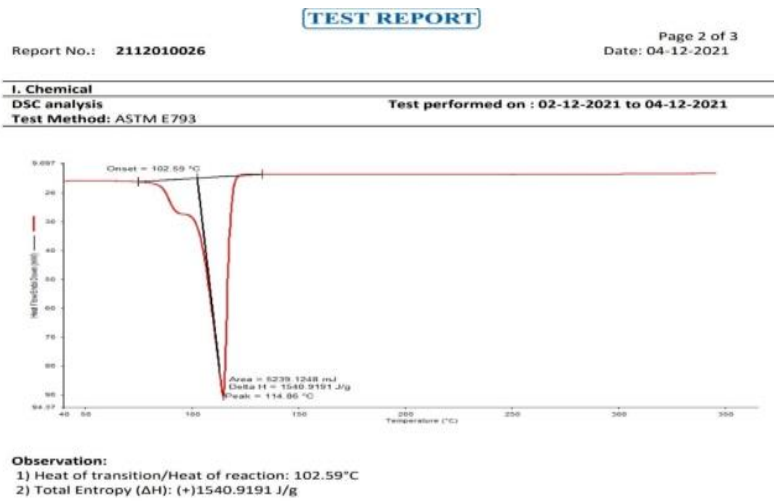
**6. Entrapment efficiency (EE %)**

The amount of the material that was trapped and utilised to determine the EE. The following formula was used to calculate the EE:

$$EE \text{ in percentage} = W2 - W1 / W1 \times 100$$

W1 = Entrapped drugs weight, W2 = Total weight of the drugs used [34].

S.No	Formulation Code	Absorbance	Entrapped Drug Conc.	DILUTION FACTOR (10)	TOTAL FORMULATION (20ML)	TOTAL FORMULATION (20ML)	ENTRAPMENT	%EE
1	C1	1.409	8.968710889	89.68710889	1.793742178	10	820.6257822	82.06257822
2	C2	1.201	7.667083855	76.67083855	1.533416771	10	846.6583229	84.66583229
3	C3	0.91	5.846057572	58.46057572	1.169211514	10	883.0788486	88.30788486



**TEST REPORT**

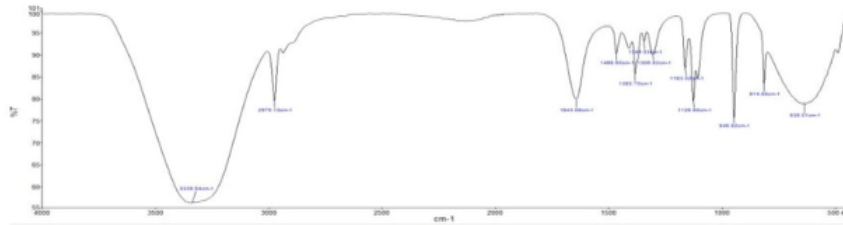
Report No.: **2112010026**

Page 3 of 3  
Date: 04-12-2021

**II. Chemical**  
**2.**

**FTIR ANALYSIS**  
Test Method: ASTM E1252:2013

Test performed on : 02-12-2021 to 04-12-2021

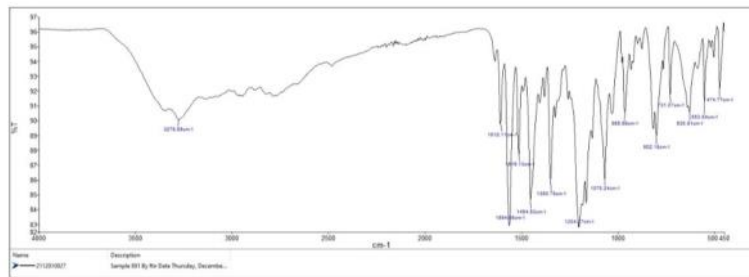


can QR code to get original data.

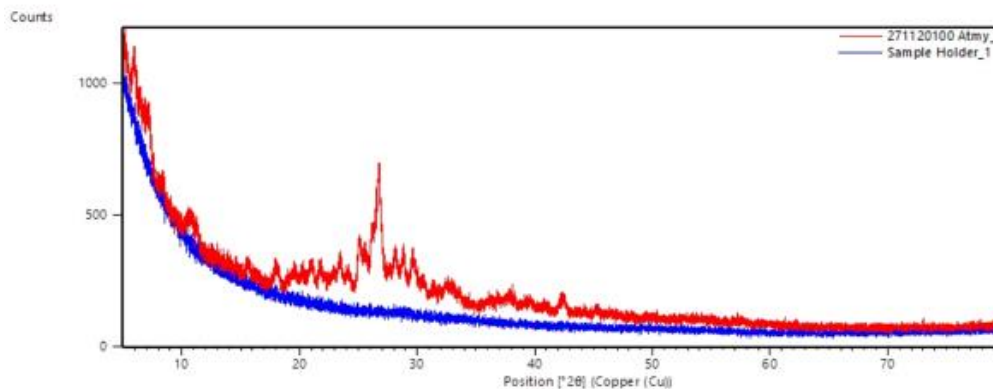
**Observation:** The given sample is scanned by FTIR Spectrum Two Perkin Elmer in which observed peaks are 3339.54cm<sup>-1</sup>, 2975.10cm<sup>-1</sup>, 1643.06cm<sup>-1</sup>, 1466.60cm<sup>-1</sup>, 1383.70cm<sup>-1</sup>, 1344.03cm<sup>-1</sup>, 1305.82cm<sup>-1</sup>, 1163.02cm<sup>-1</sup>, 1126.80cm<sup>-1</sup>, 946.82cm<sup>-1</sup>, 814.68cm<sup>-1</sup>, 635.01cm<sup>-1</sup>.

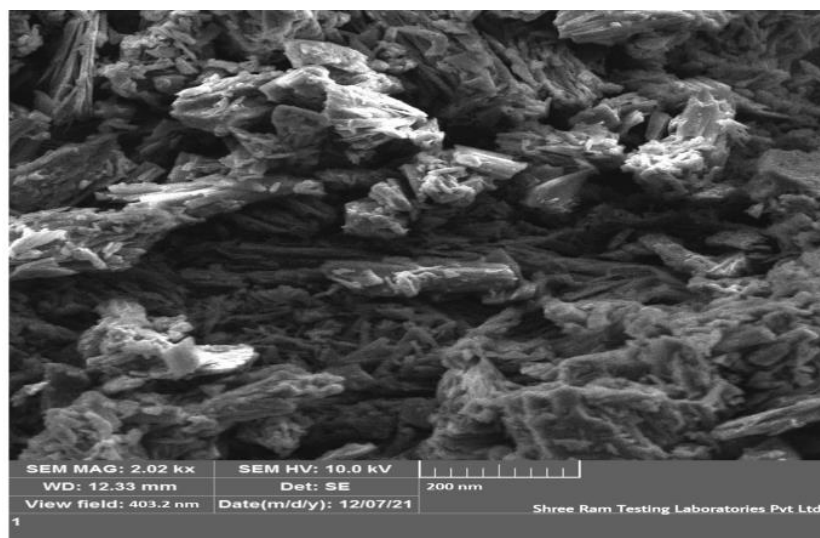
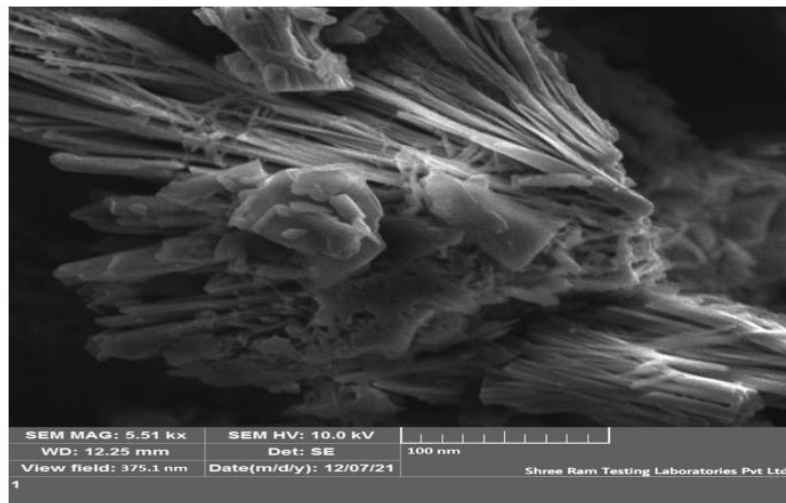
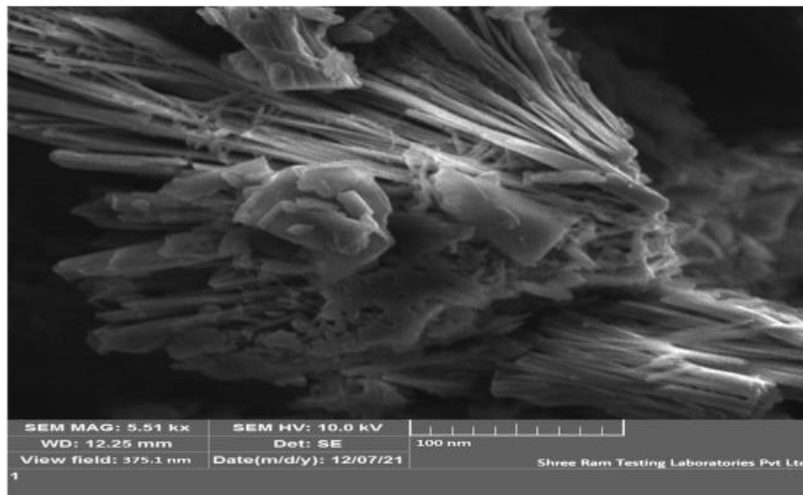
**FTIR ANALYSIS**  
Test Method : ASTM E 1252:2013

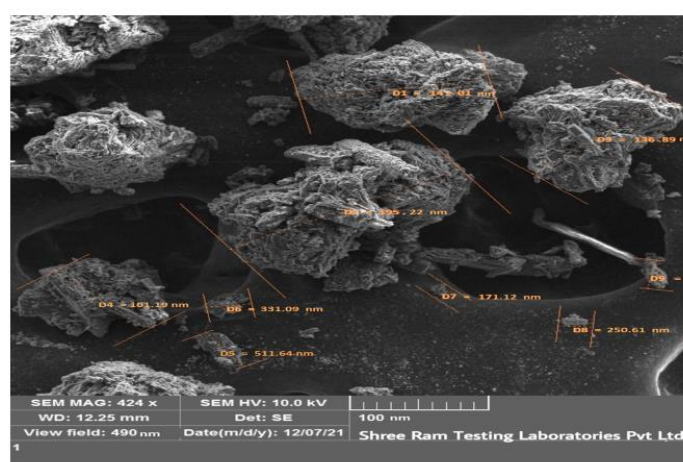
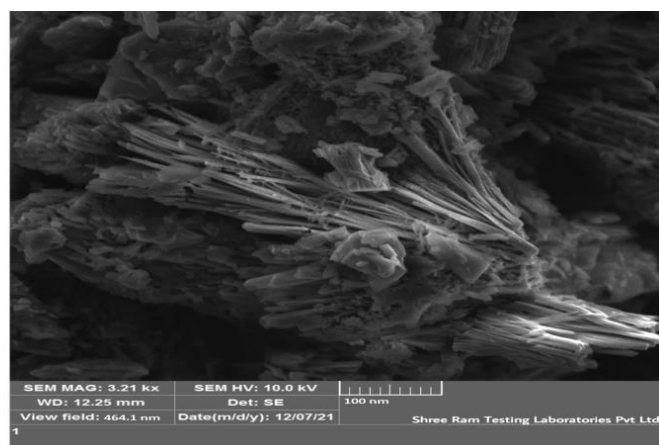
Test performed on : 03-12-2021 to 06-12-2021



**Observation:** The given sample is scanned by FTIR Spectrum Two Perkin Elmer in which observed peaks are 3276.66 cm<sup>-1</sup>, 1610.11 cm<sup>-1</sup>, 1564.06 cm<sup>-1</sup>, 1515.13 cm<sup>-1</sup>, 1454.53 cm<sup>-1</sup>, 1350.79 cm<sup>-1</sup>, 1204.27 cm<sup>-1</sup>, 1070.24 cm<sup>-1</sup>, 965.66 cm<sup>-1</sup>, 802.18 cm<sup>-1</sup>, 731.07 cm<sup>-1</sup>, 630.91 cm<sup>-1</sup>, 553.84 cm<sup>-1</sup>, 474.77 cm<sup>-1</sup>.







### 7. In-vitro release studies

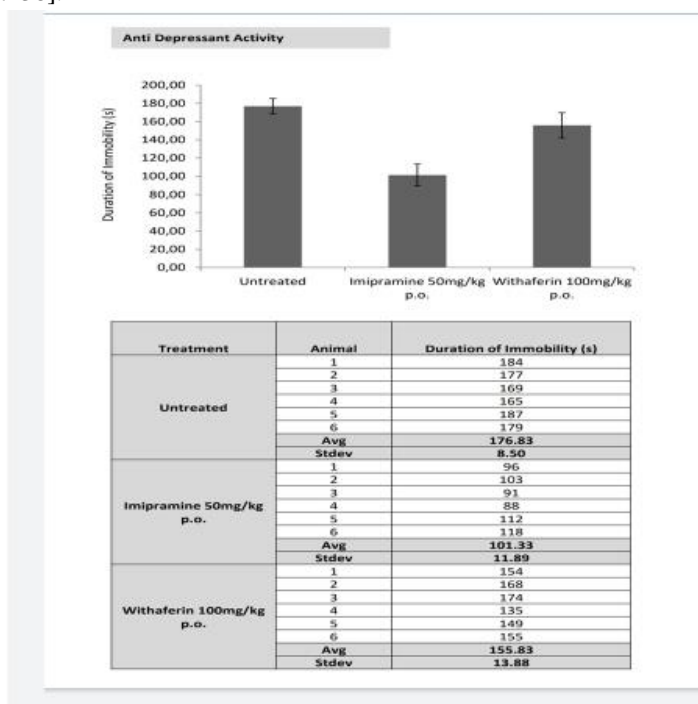
An adapted Franz diffusion apparatus was applied to test the in vitro release of nanoparticles at 32 °C. Nanoparticles corresponding to 50 mg of medication were dispersed in a phosphate buffer solution in a donor compartment. By routinely sampling 5ml of the receptor media, phosphate buffer solution, drug release was ascertained. Fresh buffer was added in its place at PH 7.4. Membrane filter with sieve number 0.22 was used to filtered the samples and a 325 nm RP-HPLC method was used to calculate the quantity of medication released [35-36].

#### 7.1 In-vivo evaluation studies

S. No.	Activity	Brief Assay design	Deliverables
1	<b>Anti depressant activity</b>	Forced swim test, single sample, single dose, n3	Duration of immobility (s), data , graphs and raw values
2	<b>Anti anxiety activity</b>	Elevated plus maze assay, single sample, single dose, n3	Time and entries in open arm data, graphs and raw values
3	<b>Blood brain barrier crossing assay</b>	Drug administered by IP route Test sample estimated in serum and brain at single end point by HPLC, single sample, single dose n1	HPLC AUC values, comparison graph between serum and brain drug levels.

## 7.2 Anti-depressant activity via a forced swim test (FST)

Minor adjustments were made to the forced swim test (FST) procedure in accordance with Porsolt's instructions. The FST test was conducted using an open cylindrical vessel that had a 14 cm radius and 20 cm in height. A depth of 15 cm and a temp. of 25<sup>o</sup>C of water were placed within the container. Mice were subjected to the test on Days 4 and 7, as well as an hour after the medication was administered. The animals' immobility period in FST was calculated as soon as they stopped wriggling and stayed still in the used water. The mice animal were made to swim or dip for 6 min, and their motionlessness was monitored. After each FST, fresh water was added to the containers [37-38].



Anti-anxiety study: The anti-anxiety investigations were conducted on Balb/c mice. All animals were randomly separated into three groups of six each. The control group given a water + (5%) Tween 80, 10 mL per kg, as the vehicle treatment. Diazepam 2 mg per kg, orally was given to the treatment groups, as the positive control group. The third group, designated as the Test Group, received the WA Test sample [39-40].

Three groups of six animals each were formed by randomly dividing the animals into groups. Animals in Group 1 (vehicle-treated control) received vehicle (10 mL/kg, diluted water + Tween 80 (5%)), 1 hour before light/dark and elevated plus maze (EPM) test for anxiety). The animals in Group 2 received diazepam (2 mg per kg, oral) 30 minute before being subjected to anxiety test. The test specimen withaferin was given to the 3<sup>rd</sup> group of animals one hour prior to the elevated plus maze test [41-42].

Model of the elevated plus-maze: Rodent anxiolytic impact was examined using the EPM test. The EPM features is 2-arms open (50 cm x 10 cm) and 2-arms closed with an open ceiling (50 cm x 10 cm x 40cm). After taking medications orally, the rat was put in the middle of the labyrinth, facing arm open, for 1 hr. at a height of 50 cm.

The treatment schedule was given following:

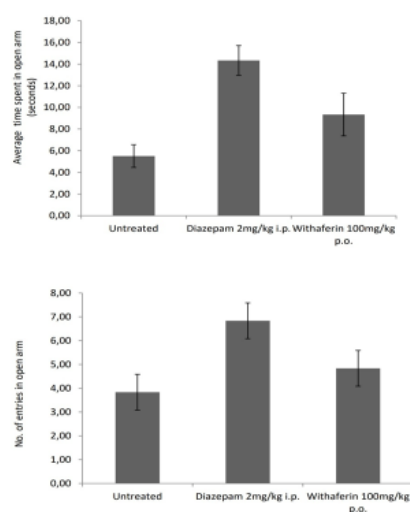
Grp. 1: Vehicle Control – One hr. before giving to the test compound

Grp. 2: Positive Control – Thirty min. before giving to the test compound

Grp. 3: Treatment Group – One hr. before giving to the test compound

A 5-minute test period was used to determine the entire number of interventions in open arms and the estimated time the animal stayed in them (average time is equal to the total time in open arms upon no. of entries in open arms) [43-44]. Across the experiment, the animals were free to interact with one another. After each test, the arena was cleaned with 5% alcohol to remove any potential bias brought on by the stench of the prior animal. Every safety measure was taken to guarantee that no outside stimuli may make the animals anxious [45-46].

Anti Anxiety Activity



Treatment	Animal	Average time spent in open arm (seconds)	No. of entries in open arm
Untreated	1	5	3
	2	4	4
	3	6	4
	4	7	5
	5	5	4
	6	6	3
	<b>Avg</b>	<b>5.50</b>	<b>3.83</b>
	<b>Stdev</b>	<b>1.05</b>	<b>0.75</b>
Diazepam 2mg/kg i.p.	1	12	6
	2	14	7
	3	16	7
	4	15	6
	5	14	8
	6	15	7
	<b>Avg</b>	<b>14.33</b>	<b>6.83</b>
	<b>Stdev</b>	<b>1.37</b>	<b>0.75</b>
Withaferin 100mg/kg p.o.	1	10	5
	2	8	5
	3	8	4
	4	7	4
	5	12	5
	6	11	6
	<b>Avg</b>	<b>9.33</b>	<b>4.83</b>
	<b>Stdev</b>	<b>1.97</b>	<b>0.75</b>

### 7.3 Brain estimation of Withaferin:

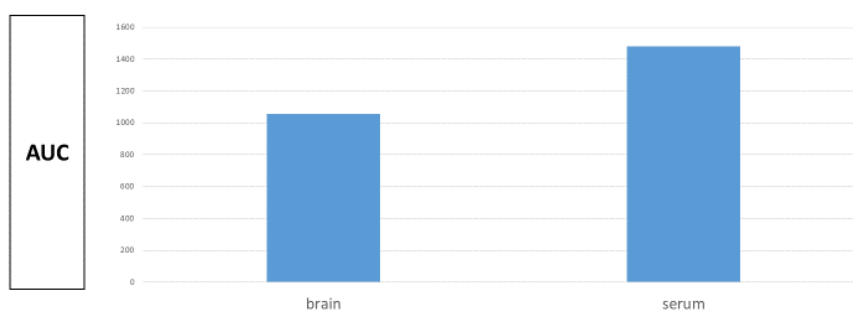
Withaferin, 1000 mg/kg, was given to the test subject. For two hours, the animal had unrestricted access to food and water. The animal was gently scarified after two hours, and blood was extracted using a terminal heart puncture. The blood plasma was precipitated using methanol. The brain was kept on ice for future analysis. The brain was centrifuged at 5000 rpm for ten minutes while being homogenized at 1g/ml. The supernatant was recovered, then methanol was used to precipitate it. Employing HPLC, the supernatants were examined. HPLC was used by using a Shimadzu Prominence that involved a CBM-20A communication bus module, LC-20AT quaternary gradient pump, CTO-10AS column furnace, SIL-20AC autosampler, and Shimadzu LC software version 1.21 SP1. Filters measuring 0.45 m (Millipore) that were imported from India were used to filter each of the specimens and standards. The samples were separated using Merck's Microsphere column, which has 250 mm x 4.6 mm i.d. 5 μm-sized particles. Acetonitrile and water were used in the isocratic elution process as a mobile phase with the flow speed of 0.8 ml per minute. The temperature of the column's was held constant at 27°C. The analytes were detected at Rt 6.9 minutes using the SPD-M20A photodiode array detector [47–48].

#### Withaferin estimation in Brain

Withaferin concentration (AUC) in brain 2 hours post administration		
Treatment	Brain	Serum
Withaferin 1000 mg/kg i.p.	1058	1478
Withaferin Standard 0.001 ug/ml		12654

Parameter	Specification
Pump	LC-20AT quaternary gradient pump
Column	Licrosphere column (250 mm x 4.6 mm i.d. 5 μm particle size) from Merck
Mobile Phase	acetonitrile: water (45:55 v/v)
Elution Mode	isocratic elution
flow rate	0.8 mL/min
The column temperature	27°C
Detection of analytes	Rt 6.9 minutes
Abs detection	225 nm



## 8 Conclusion

Transporting common anti-neurotic compounds like WA was effectively using the combined nano- formulation of PVA, non-ionic surfactant Tween 80, and eudragit. The WA was confined in amorphous forms, as shown by DSC, and the drug molecule next to it had not undergone any chemical alteration. The Nano formulation size was less than 300 nm. Over the course of a 12-hour period, the drug was continually administered by the nano-forms. The WA-nanofoms cellular collaboration identified significant anti-neurotic action in the assay of comet. What's more, these nanoparticles with hybrid exhibited much larger antineurotic efficacy in in vivo and in vitro. WA-loaded nanofoms described here might therefore assist as a model for using natural resources as therapeutics for neurological disorders, opening new opportunities to maximize the efficacy of dietary supplements.

## References

- [1]. Vishnu SS, Reshmi MKN, Abbas R, Simona B, Dana CZ, Lotfi A, Delia MT: Overview of the anticancer activity of withaferin A, an active constituent of the Indian ginseng withania somnifera; published: 13 May 2020.
- [2]. Nawab JD and Muzamil A, Neurodegenerative disease and Withania somnifera(L): An update; Journal of Ehtnopharmacology Volume 256, 28 June 2020, 112769
- [3]. Saraiva C, Praça C, Ferreira R, Santos T, Ferreira L, Bernardino L. Nanoparticle-mediated brain drug delivery: Overcoming blood-brain barrier to treat neurodegenerative diseases. Journal of Controlled Release. 2016; 235:34–47.
- [4]. Nagpal K, Singh SK, Mishra DN. Drug targeting to brain: a systematic approach to study the factors, parameters and approaches for prediction of permeability of drugs across BBB. Expert Opinion on Drug Delivery. 2013;10(7):927–55.
- [5]. Chen, Y. et al. Gut microbiome alterations precede cerebral amyloidosis and microglial pathology in a mouse model of Alzheimer's disease. Biomed. Res Int 2020, 8456596 (2020).
- [6]. Journal AI, Selvaraj K, Gowthamarajan K, Venkata V. Nose to brain transport pathways an overview: potential of nanostructured lipid carriers in nose to brain targeting. Artificial Cells, Nanomedicine, and Biotechnology [2017]
- [7]. Vivienne A, Chris HT, Rui S, Nan L, Priestley RD. Nanomedicine as a non-invasive strategy for drug delivery across the blood brain barrier. International Journal of Pharmaceutics. 2016.
- [8]. Chen W, Zuo H, Zhang E, Li L, Henrich-Noack P, Cooper HM, et al. Brain targeting delivery facilitated by ligand-functionalized layered double hydroxide nanoparticles. ACS Applied Materials and Interfaces. 2018.
- [9]. Boronic B, Modi E. Bioengineered Boronic Ester Modi fi ed Dextran Polymer Nanoparticles as Reactive Oxygen Species Responsive Nanocarrier for Ischemic Stroke Treatment. 2018;
- [10]. Zhao X, Shang T, Zhang X, Ye T, Wang D, Rei L. Passage of Magnetic Tat-Conjugated Fe3O4@SiO2 Nanoparticles Across In Vitro Blood-Brain Barrier. Nanoscale Research Letters [Internet]. 2016;11.
- [11]. Rohit Bhandari; pal, kaur indu, A method to prepare solid lipid nanoparticles with improved entrapment efficiency of hydrophilic drugs; Volume 9, Number 2, 2013, pp. 211-220(10)

- 
- [12]. Taranjeet K, Harpal S, Rachana M, Shaffi M, Muskan G, Vadangana S, Anuradha S and Gurcharan K ; Withanai somnifera as a potential anxiolytic and immunomodulatory agent in acute sleep deprived female wistar rats; *Molecular and cellular biochemistry* 427, pages91–101 (2017).
- [13]. Laperle AH, Sances S, Yucer N, Dardov VJ, Garcia VJ, Ho R, et al. iPSC modeling of young-onset Parkinson's disease reveals a molecular signature of disease and novel therapeutic candidates. *Nat Med.* 2020.
- [14]. Sen T, Saha P, Gupta R, Foley LM, Jiang T, Abakumova OS, et al. Aberrant ER stress induced neuronal-IFNbeta elicits white matter injury due to microglial activation and T-cell infiltration after TBI. *J Neurosci.* 2020.
- [15]. Benichou, G., Wang, M., Ahrens, K. & Madsen, J. C. Extracellular vesicles in allograft rejection and tolerance. *Cell Immunol.* 349, 104063. <https://doi.org/10.1016/j.cellimm.2020.104063> (2020).
- [16]. Hassannia, B., Logie, E., Vandenabeele, P., Vanden Berghe, T. & Vanden Berghe, W. Withaferin A: From ayurvedic folk medicine to preclinical anti-cancer drug. *Biochem Pharmacol* 173, 113602. <https://doi.org/10.1016/j.bcp.2019.08.004> (2020).
- [17]. Dutta, R., Khalil, R., Green, R., Mohapatra, S. S. & Mohapatra, S. Withania somnifera (Ashwagandha) and withaferin A: Potential in integrative oncology. *Int. J. Mol. Sci.* <https://doi.org/10.3390/ijms20215310> (2019).
- [18]. McKinsey, T. A., Chu, Z., Tedder, T. F. & Ballard, D. W. Transcription factor NF-kappaB regulates inducible CD83 gene expression in activated T lymphocytes. *Mol. Immunol.* 37, 783–788. [https://doi.org/10.1016/s0161-5890\(00\)00099-7](https://doi.org/10.1016/s0161-5890(00)00099-7) (2000).
- [19]. Pabst, G., Rappolt, M., Amenitsch, H. & Laggner, P. Structural information from multilamellar liposomes at full hydration: Full q-range fitting with high quality X-ray data. *Phys. Rev. E* 62, 4000 (2000).
- [20]. Pandian, B. A., Sathishraj, R., Djanaguiraman, M., Prasad, P. V. V. & Jugulam, M. Role of cytochrome P450 enzymes in plant stress response. *Antioxidants* 9, 454 (2020).
- [21]. Mizrahi, J. D., Surana, R., Valle, J. W. & Shroff, R. T. Pancreatic cancer. *Lancet* 395(10242), 2008–2020 (2020).
- [22]. Piffoux, M., Eriau, E. & Cassier, P. A. Autophagy as a therapeutic target in pancreatic cancer. *Br. J. Cancer.* 124(2), 333–344 (2021).
- [23]. Yue, P. et al. Development of an autophagy-related signature in pancreatic adenocarcinoma. *Biomed. Pharmacother.* 126, 110080 (2020).
- [24]. Lin, Z. et al. Pan-cancer analysis of genomic properties and clinical outcome associated with tumor tertiary lymphoid structure. *Sci. Rep.* 10, 21530 (2020).
- [25]. Zhou, C., Li, A.H., Liu, S., Sun, H. Identification of an 11-Autophagy-related-gene signature as promising prognostic biomarker for bladder cancer patients. *Biology (Basel).* 2021.
- [26]. Ren, Z. et al. Development and validation of a novel survival model for head and neck squamous cell carcinoma based on autophagy-related genes. *Genomics* 113(1 Pt 2), 1166–1175 (2021).
- [27]. Jin, Y. & Qin, X. Development of a prognostic signature based on autophagy-related genes for head and neck squamous cell carcinoma. *Arch. Med. Res.* 51(8), 860–867 (2020).
- [28]. Yang, C. et al. Prognostic correlation of an autophagy-related gene signature in patients with head and neck squamous cell carcinoma. *Comput. Math. Methods Med.* 2020, 7397132 (2020).
- [29]. Hu, D. et al. Development of an autophagy-related gene expression signature for prognosis prediction in prostate cancer patients. *J. Transl. Med.* 18(1), 160 (2020).
- [30]. Kögel, D., Linder, B., Brunschweiler, A., Chines, S., Behl, C. At the crossroads of apoptosis and autophagy: Multiple roles of the co-chaperone BAG3 in stress and therapy resistance of cancer. *Cells.* 2020.
- [31]. Raffone, A. et al. BAG3 expression correlates with the grade of dysplasia in squamous intraepithelial lesions of the uterine cervix. *Acta Obstet. Gynecol. Scand.* 99(1), 99–104 (2020).
- [32]. Zhuang, H. et al. A four prognosis-associated lncRNAs (PALnc) based risk score system reflects immune cell infiltration and predicts patient survival in pancreatic cancer. *Cancer Cell Int.* 20, 493 (2020).

- 
- [33]. Wu, J. et al. TNFSF9 promotes metastasis of pancreatic cancer through Wnt/Snail signaling and M2 polarization of macrophages. *Aging (Albany NY)* 13, 21571–21586 (2021).
- [34]. Boor, P. et al. HHLA2 is expressed in pancreatic and ampullary cancers and increased expression is associated with better post-surgical prognosis. *Br. J. Cancer* 122, 1211–1218 (2020).
- [35]. Xiang, H. et al. Targeting autophagy-related protein kinases for potential therapeutic purpose. *Acta Pharm. Sin B.* 10(4), 569–581 (2020).
- [36]. Liang, C. et al. TGFB1-induced autophagy affects the pattern of pancreatic cancer progression in distinct ways depending on SMAD4 status. *Autophagy* 16(3), 486–500 (2020).
- [37]. Matrood, S., de Prisco, N., Wissniowski, T., et al. Modulation of pancreatic neuroendocrine neoplastic cell fate by autophagy mediated death. *Neuroendocrinology*. 2020.
- [38]. Xiang, H. et al. Targeting autophagy-related protein kinases for potential therapeutic purpose. *Acta Pharm. Sin B.* 10(4), 569–581 (2020).
- [39]. Liang, C. et al. TGFB1-induced autophagy affects the pattern of pancreatic cancer progression in distinct ways depending on SMAD4 status. *Autophagy* 16(3), 486–500 (2020).
- [40]. Matrood, S., de Prisco, N., Wissniowski, T., et al. Modulation of pancreatic neuroendocrine neoplastic cell fate by autophagy mediated death. *Neuroendocrinology*. 2020.
- [41]. Tang, Q. et al. Withaferin A triggers G2/M arrest and intrinsic apoptosis in glioblastoma cells via ATF4-ATF3-CHOP axis. *Cell Prolif.* 53, e12706 (2020).
- [42]. Xie, Z. et al. Expression of N6-methyladenosine (m6A) regulators correlates with immune microenvironment characteristics and predicts prognosis in diffuse large cell lymphoma (DLBCL). *Bioengineered* 12, 6115–6133. (2021).
- [43]. Liu, J. Q. et al. CD200-CD200R pathway in the regulation of tumor immune microenvironment and immunotherapy. *Adv. Exp. Med. Biol.* 1223, 155–165. [https://doi.org/10.1007/978-3-030-35582-1\\_8](https://doi.org/10.1007/978-3-030-35582-1_8) (2020).
- [44]. Arjuna, H. & Guillerey, C. TIGIT as an emerging immune checkpoint. *Clin. Exp. Immunol.* 200, 108–119. <https://doi.org/10.1111/cei.13407> (2020).
- [45]. Kanehisa, M., Furumichi, M., Sato, Y., Ishiguro-Watanabe, M. & Tanabe, M. KEGG: Integrating viruses and cellular organisms. *Nucl. Acids Res.* 49, D545–D551 (2021).
- [46]. Chen, G. et al. Identification of key signaling pathways and genes in eosinophilic asthma and neutrophilic asthma by weighted gene co-expression network analysis. *Front. Mol. Biosci.* 9, 805570 (2022).
- [47]. Zhang, Q. et al. Identification of an autophagy-related pair signature for predicting prognoses and immune activity in pancreatic adenocarcinoma. *Front. Immunol.* 12, 5073 (2021).
- [48]. Paszek, M. & Tukey, R. H. NRF2-independent regulation of intestinal constitutive androstane receptor by the pro-oxidant's cadmium and isothiocyanate in hUGT1 mice. *Drug Metab. Dispos.* 48, 25–30 (2020).